GFZ
Helmholtz-Zentrum
POTSDAM

Originally published as:

Ziabakhsh-Ganji, Z., Nick, H. M., Donselaar, M. E., Bruhn, D. (2018): Synergy potential for oil and geothermal energy exploitation. - *Applied Energy*, *212*, pp. 1433—1447.

DOI: http://doi.org/10.1016/j.apenergy.2017.12.113

Applied Energy 212 (2018) 1433–1447

Contents lists available at ScienceDirect

Applied Energy

journal homepage: www.elsevier.com/locate/apenergy

Synergy potential for oil and geothermal energy exploitation

Zaman Ziabakhsh-Ganji[a,*], Hamidreza M. Nick[a,b], Marinus E. Donselaar[a], David F. Bruhn[a,c]

[a] Faculty of Civil Engineering and Geosciences, Delft University of Technology, The Netherlands
[b] Danish Hydrocarbon Research and Technology Centre, Technical University of Denmark, Denmark
[c] Helmholtz Centre Potsdam – GFZ German Research Centre for Geosciences, Germany

HIGHLIGHTS

- Detailed study on combining geothermal energy and thermally enhanced oil recovery.
- Combining these projects can reduce the required subsidy for geothermal projects.
- Wellbore spacing plays a key role in oil recovery and geothermal energy performance.
- Effectiveness of enhanced oil production strongly depends on the heat plume shape.

GRAPHICAL ABSTRACT

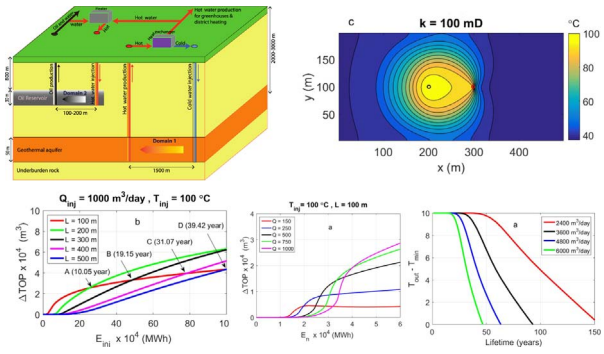

ARTICLE INFO

Keywords:
Non-isothermal flow
Geothermal doublet
Thermal enhanced heavy oil recovery
Energy production
Heat plume
Net present value

ABSTRACT

A new solution for harvesting energy simultaneously from two different sources of energy by combining geothermal energy production and thermal enhanced heavy oil recovery is introduced. Numerical simulations are employed to evaluate the feasibility of generating energy from geothermal resources, both for thermally enhanced oil recovery from a heavy oil reservoir and for direct heating purposes. A single phase non-isothermal fluid flow modeling for geothermal doublet system and a two-phase non-isothermal fluid flow modelling for water flooding in an oil reservoir are utilised. Sensitivity and feasibility analyses of the synergy potential of thermally-enhanced oil recovery and geothermal energy production are performed. A series of simulations are carried out to examine the effects of reservoir properties on energy consumption and oil recovery for different injection rates and injection temperature. Our results show that total oil production strongly depends on the shape of heat plume which can be affected by porosity, permeability, injection temperature, well spacing and injection rate in the oil reservoir. The favourable oil recovery obtains at high amount of (a) injection rate, (b) injection temperature, (c) porosity and (d) low amount of oil reservoir permeability respectively. Furthermore, our study indicates the wellbore spacing plays an important role in oil recovery and an optimum wellbore spacing can be established. The analyses suggest that the extra amount of oil produced by utilising the geothermal energy could make the geothermal business case independent and may be a viable option to reduce the overall project cost. Furthermore, the results display that the enhance oil productions are able to reduce the required subsidy for a single doublet geothermal project up to 50%.

* Corresponding author.
E-mail address: z.ziabakhshganji@tudelft.nl (Z. Ziabakhsh-Ganji).

https://doi.org/10.1016/j.apenergy.2017.12.113
Received 14 October 2017; Received in revised form 6 December 2017; Accepted 30 December 2017
0306-2619/ © 2018 The Author(s). Published by Elsevier Ltd. This is an open access article under the CC BY license (http://creativecommons.org/licenses/BY/4.0/).

Nomenclature

$\Delta\dot{E}_i$	annual thermal energy extracted
$\dot{m}_i$	mass production of hot water
c_p	specific heat
ΔT_i	temperature difference between the produced and injected
ρC	volumetric heat capacity
q'	external sinks and sources
T'	temperature at sources
P	pressure
$\boldsymbol{u}$	Darcy velocity vector
k	permeability
k_{ro}	oil relative permeability
k_{rw}	water relative permeability
S_{orw}	residual oil saturation
S_{wir}	initial water saturation
ΔTOP	total oil production variable (TOP for elevated Temperature injection – TOP for T_{inj} = 37 °C)
S	salinity of geothermal fluid
Q	injection rate in oil reservoir
L	distance between injection and production wells in oil reservoir domain
GWh	gigawatt hour
E_{inj}	energy injection in oil reservoir domain
E_n	net cumulative energy consumption in oil reservoir
Q^w_{inj}	water injection rate in oil reservoir domain
Q^w_{pro}	water production rate in oil reservoir domain
T_{init}	initial temperature in oil reservoir domain
T_{inj}	injection temperature in oil reservoir domain
T_{pro}	production temperature of oil reservoir
T_s	surface temperature
NPV	net present value
S_a	brine salinity (M)
MWh	megawatt hour
γ	dynamic viscosity
μ	viscosity
ρ	density
λ	thermal conductivity
ϕ	porosity

1. Introduction

In the Netherlands geothermal energy production from deep geological formations has a great potential as environmentally benign heat source, and its usage has been growing since the first well doublets were realised in 2007 [1]. The main geothermal targets are hot sedimentary aquifers at depths between 2 and 3 km with approximately a temperature of 70–100 °C (e.g., [2]). A doublet system consisting of a hot-water production and a cold-water reinjection well can be utilised to harvest energy from the hot sedimentary aquifers (e.g., [3]). Despite recent developments and a growing number of projects in the Netherlands, however, geothermal energy is not yet cost-competitive without subsidies.

Many of the geothermal reservoirs identified and currently used in the hot sedimentary aquifers of the Netherlands are in close proximity and often from the same reservoir rocks as the well-characterised hydrocarbon resources of the country. And even though these oil and gas reservoirs have been exploited successfully for many decades, not all of the known resources have been produced, some reservoirs have even been abandoned for various reasons. An example of an abandoned oil reservoir is the Moerkapelle field in the West Netherlands Basin, which contains highly viscous heavy oil at approximate 850 m depth. The viscosity of the oil was simply too high to be produced economically.

One way to produce heavy oil is by hot water or steam injection. While this method of enhanced oil recovery (EOR) is routinely applied all over the world it is not always energetically or economically viable. In the case of the Moerkapelle field, operations were stopped because the viscosity of the oil in the reservoir was so high and the reservoir is relatively small such that standard EOR approaches available at the time did not help to produce enough of the available oil. For this reason, the field was abandoned in1986.

In this paper, the synergy potential of a combined energy production from a geothermal reservoir and the heavy oil from the Moerkapelle field is investigated employing numerical simulations. The geothermal reservoir will provide the hot water for flooding of the oil reservoir as well as for the heating of greenhouses or other buildings nearby. The oil produced could make the overall project economically feasible: the hot water makes oil production possible and the co-produced oil could make the geothermal business case independent of subsidies. To perform such a study, both parameters that control the efficiency and productivity of a geothermal reservoir and those making heavy oil production feasible and profitable are examined.

Hot water flooding as a key method for thermal enhanced heavy oil recovery, is utilised routinely in the oil and gas industries [4]. Many authors [5–7] suggested that the most effective methods are steam flooding or hot water flooding resulting in an enhanced recovery factor of about 20–30%. Numerous laboratory experiments and numerical simulation studies have shown that the oil viscosity and mobility ratio can be reduced by hot water injection, resulting in ultimately resulting in improved oil recovery (e.g., [8–12]). Martin et al. [13], considering a case study of a hot water flood pilot test in the Loco field in southern Oklahoma which contains crude oil with 600 cp viscosity, showed the hot water flooding yield oil recovery increasing. In another case study, Cassinat et al. [14] showed hot water injection may significantly increase pool recoveries as much as 25% in the Senex oil field located in Northern Alberta, Canada, which contains a 12 cp (37° API) crude with high paraffin content. Yu [15] showed that when injecting cold water to displace oil, the injected cold water cools down the oil layer which increases the oil viscosity and changes the oil-water phase permeability. These changes result in an oil displacement efficiency reduction of 2–8%. Pederson and Sitorus [16], Wang and Wang [17], and Chen et al. [18] indicated that thermal water flooding is superior to conventional water flooding, and can improve oil recovery by 4–10%.

While in most cases the hot water for thermal water flooding is produced by burning fossil fuels, a geothermal reservoir could provide an economically and environmentally promising alternative to provide steam or hot water. Abandoned deep-hydrocarbon reservoirs and dry wells also have been considered as geothermal energy source [19]. Simulation studies of hot water injection in heavy oil reservoirs (and its effects on oil reservoir behaviour) and of geothermal doublet performances are individually well developed [3,20–27]. Investigations combining the geothermal energy sources and heavy oil reservoirs, however, are still limited.

To our knowledge, this option has only been tested once so far by Wys et al. [28], who conducted an economic feasibility study on recovering heavy oil using a geopressured geothermal resource in an oilfield of south Texas. The study showed that the breakeven price for oil is less than 14 dollars per barrel and for gas less than 2 dollars per thousand cubic feet and the payback is less than 2 years after injection [29]. They suggested that such an application is profitable for heavy oil recovery enhancement. However, they did not consider some controlling parameters such as wellbore distance, injection rate and injection temperature on the oil recovery.

In this study, the feasibility of generating energy from geothermal resources, both for EOR from a heavy oil reservoir and for heating purposes is addressed through a numerical study. The parameters of a

specific site are utilised. And the sensitivity of the system to several injection parameters, such as well distance, injection temperature and injection and production rates is explored.

The aim of the present study is to assess and develop new strategies for integration of geothermal energy with heavy oil production from a stranded oil field. To this end, we develop a model involving the solution of a nonlinear conduction-convection heat transport and two phase fluid flow occurring in porous media to analyse the key parameters such as porosity, permeability and the injection rate/temperature in the oil reservoir and also how these parameters could control the ultimate heavy oil recovery, sweep efficiency and the geothermal energy consumption.

2. Methodology

In the Netherlands the Westland area has the highest density of greenhouses, several of which are heated by geothermal energy. The reservoir is usually a porous sandstone from the Lower Cretaceous Nieuwekerk formation in the West Netherlands Basin. Many hydrocarbon fields in the Netherlands are either abandoned or are not developed due to being non-profitable such as Moerkapelle [30–32]. The Moerkapelle field (white lines in Fig. 1), located about 15 km northeast of the city of Delft, is a heavy oil field in the lower Cretaceous Delft Sandstone at a depth of about 800–1000 m. Petrophysical analysis of the logs from the Moerkapelle wells provided average properties for the Delft Sandstone, which are listed in Table 1. Below of this stranded field at depth between 2 and 3 km, there is a sedimentary aquifer (geothermal reservoir) with approximately a temperature of 70–100 °C, which can be utilised for enhanced thermal heavy oil recovery.

The simulation study shown in Fig. 2 consists of two domains: (1) a geothermal doublet (single phase flow model) and (2) a heavy oil (two-phase flow model) reservoir.

For the geothermal model (Domain 1 in Fig. 2), similar to Willems et al. [33], a three dimensional (3D) finite element method implemented in COMSOL Multiphysics is utilised to simulate fluid flow and heat transfer processes in geothermal doublets which consist of a cold water injection well and a hot water production well. This provides the data for the calculation of the doublet performance. The results generated from the geothermal simulation are obtained assuming that connectivity and net to gross (N/G) ratio of the sandstone reservoir are both 100%. Three layers (each with 50 m thickness) are simulated in Domain 1: Overburden, geothermal aquifer and underburden. The model size is 2000 m × 1000 m × 150 m. An injection temperature of

Table 1
List of parameters used in the geothermal model Domain 1.

Parameters	Value	Dimension	Description
T_0	100	°C	Initial reservoir temperature
T_{inj}	37	°C	Injection cold water temperature
P_0	20	MPa	Initial reservoir pressure
Cp_f	4200	J/(kg K)	Specific heat capacity of the fluid
λ_f	0.67	W/(m K)	Conductivity of the pore fluid
S	0.02	ppm/10^6	Salinity of the injection fluid
α_T	0.001	m	Transversal dispersion coefficient
α_L	0.01	m	Longitudinal dispersion coefficient
r_w	0.075	m	Wellbore radius
ϕ_{res}	0.28	–	Porosity
λ_s	3	W/(m K)	Conductivity of the reservoir rock
ρ_s	2650	kg/m^3	Density of the reservoir rock
Cp_s	980	J/(kg K)	Specific heat capacity of the reservoir rock
k_{res}	1000	mD	Permeability of the reservoir
Adjacent layer (over and underburden)			
ρ_{adj}	2600	kg/m^3	Density of the adjacent (over and underburden) rock
λ_{adj}	2.0	W/(m K)	Conductivity of the rock
Cp_{adj}	950	J/(kg K)	Specific heat capacity of the rock
ϕ_{adj}	0.05	–	Porosity
k_{adj}	0.01	mD	Permeability

Fig. 1. Greenhouses agriculture (potential geothermal energy users) around the Moerkapelle village and the oil field (white lines).

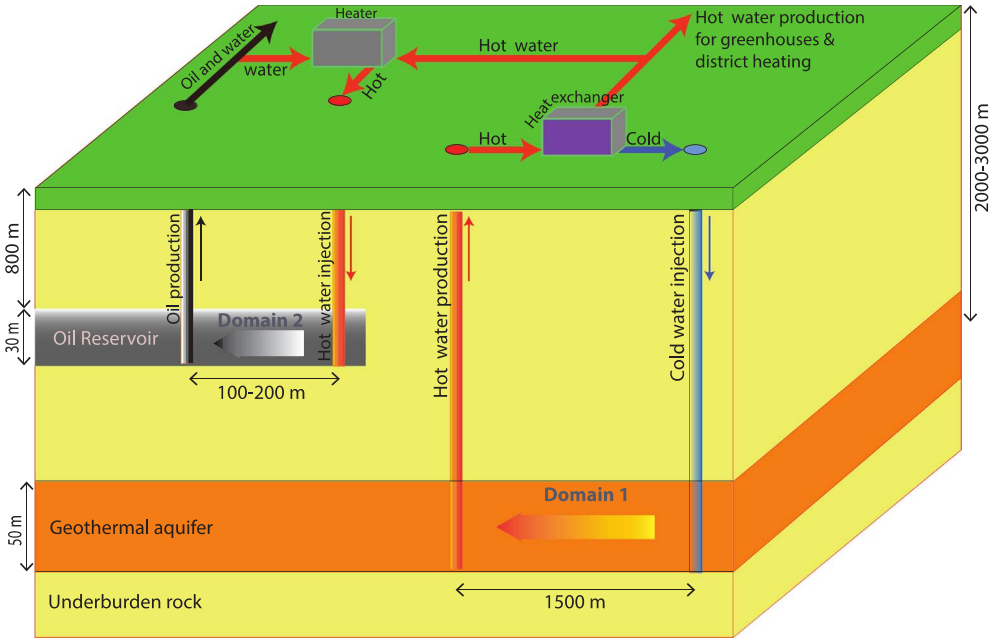

Fig. 2. Schematic of the conceptual model and simulation study domains. The arrows next to the wells represent the flow direction. The geothermal well distance is 1500 m while different well distances ranging from 100 m to 500 m are examined for Domain 2.

Table 2
List of parameters used in the Moerkappelle oil field model Domain 2.

Parameters	Value	Dimension	Description
T_0	37	°C	Initial oil reservoir temperature
P_0	8.96	MPa	Initial reservoir pressure
ϕ_{res}	0.18	–	Porosity
Cp_w	4190	J/(kg K)	Specific heat capacity of the water phase
λ_w	0.67	W/(m K)	Conductivity of the water phase
k_{res}	496	mD	Permeability of the reservoir
r_w	0.075	m	Wellbore radius
h	30	m	Reservoir thickness
GOR	16	m^3/m^3	Initial solution gas oil ratio
λ_{rock}	3	W/(m K)	Conductivity of the reservoir rock
ρ_{rock}	2650	kg/m^3	Density of the reservoir rock
Cp_r	980	J/(kg K)	Specific heat capacity of the reservoir rock
Cp_o	2012	J/(kg K)	Specific heat capacity of the oil phase
c_r	5E-4	psi^{-1}	Formation compressibility
c_o	5E-6	psi^{-1}	Oil compressibility
S_{oi}	0.83	–	Initial oil saturation
λ_o	0.18	W/(m K)	Thermal conductivity of the oil
λ_r	3	W/(m K)	Thermal conductivity of reservoir Rock
λ_w	0.67	W/(m K)	Thermal conductivity of water phase
OOIP	44.874×10^4	m^3	Original oil in place
Adjacent layers (over and underburden)			
$\lambda_{r,over}$	2.2	W/(m K)	Thermal conductivity of overburden caprock
$\lambda_{r,under}$	2.2	W/(m K)	Thermal conductivity of underburden caprock
$Cp_{r,over}$	920	J/(kg K)	Specific heat capacity of the overburden caprock
$Cp_{r,under}$	920	J/(kg K)	Specific heat capacity of the underburden caprock

37 °C (e.g. [34]) and an initial reservoir temperature of 100 °C are considered. The reservoir properties such as average porosity, permeability and reservoir rock thermal properties (Table 1) are chosen based on Crooijmans et al. [20]. It should be noted that the pore fluid used in the dynamic model is brine with a constant specific heat capacity, heat conductivity and salinity. The viscosity and density of the brine vary with temperature, the salinity of the brine and pressure [35]. The injection and the production wells have the same discharge rate (e.g. [34,36]), which remains constant over time. The two outer boundaries at the short edge are assigned a constant pressure; the others are modelled as no flow boundaries.

For the oil reservoir model (Domain 2 shown in Fig. 2), a non-isothermal two-phase flow model developed in ECLIPSE 300 is utilised to investigate the energy consumption for thermal EOR. Both models contain two wells (injection and production) and initial reservoir conditions are homogeneous (i.e. uniform porosity, permeability and reservoir rock thermal properties). With this model setup, responses for constant mass rate injection scenarios are studied. Although these conditions are clearly idealized, model simulations are considered appropriate to illustrate the essential generic features of EOR. Evaluation of detailed responses of specific reservoirs might necessitate consideration of reservoir-specific parameterizations, but these are considered beyond the scope of the present evaluation. The model for Domain 2 contains two wells of which one is used to produce heavy oil from a depth of approximately 800 m and the other serves as the injector of hot water. This hot water is provided from a geothermal reservoir (Domain 1), beneath the Moerkapelle oil field, partly pumped directly into the oil reservoir or pumped through a heat exchanger for energy extraction purposes at the surface before it is reinjected into the deep aquifer again. In Domain 2, the initial gas oil ratio (GOR) of Moerkapelle field is 16 [37], indicating that there is little light components in the oil. Due to limited access to Pressure, Volume, Temperature (PVT) information data of the reservoir fluid properties, some missing data are adapted from the Fourth Society of Petroleum Engineers (SPE) Comparative Solution Project, problem 1 [38]. Some sensitivity analyses are performed to show the impact of the adjusted reservoir fluid data on the ultimate heavy oil recovery for the Moerkapelle field. The size of the oil reservoir model, as base case scenario of the model, is $500 \times 200\,m^2$ and 30 m in thickness that includes 448,740 m^3 of crude oil as original oil in place (OOIP). The model consists of 24,000 ($100 \times 40 \times 60$) grid cells (hexahedra) in which the rock is assumed to have isotropic and homogenous properties. Thermal properties including thermal conductivity and heat capacity of rock are also assumed to be homogeneous, but different for the cap and the base rock. Table 2 summarizes grid thermal properties used in the base case model.

2.1. Geothermal reservoir (Domain 1)

Heat transfer in geothermal systems can be described with two main processes: conduction and convection. For a system with a rigid rock, incompressible fluids and local thermal equilibrium between rock and fluid the heat transfer equation reads:

$$\frac{\partial(\rho CT)}{\partial t} = \nabla\cdot(\lambda\nabla T) - \nabla\cdot(\rho_f C_f \boldsymbol{u} T) - \rho_f C_f q' T' \tag{1}$$

where t is time [s], T the temperature [K], $\boldsymbol{\lambda}$ the total conductivity tensor [W/(m K)], ρ_f the fluid density [kg/m^3], C_f the fluid specific heat capacity [J/(kg K)], $\boldsymbol{u}$ is Darcy velocity vector [m/s], and ρC is the volumetric heat capacity, q' is external sinks and sources [1/s], and T' refers to the temperature at sources/sinks. Darcy velocity is calculated as: $\boldsymbol{u} = -k/\mu\nabla P$, where μ is the dynamic viscosity [Pa s], k is permeability [mD] and P is the fluid pressure [Pa]. The fluid pressure field can be obtained by solving the continuity equation: $\phi\partial\rho_f/\partial t + \nabla.(\rho_f \boldsymbol{u}) = \rho_f q'$. The total thermal conductivity is expressed as: $\boldsymbol{\lambda} = \lambda_{eq}\boldsymbol{I} + \boldsymbol{\lambda}_{dis}$. Where λ_{eq} is the equivalent conductivity of the fluid and the matrix and the $\boldsymbol{\lambda}_{dis}$ the thermal dispersion tensor. This equivalent conductivity and the volumetric heat capacity are both volume averaged:

$$\lambda_{eq} = (1-\phi)\lambda_s + \phi\lambda_f \tag{2}$$

$$\rho C = (1-\phi)\rho_s C_s + \phi\rho_f C_f \tag{3}$$

where the suffixes s and f stand for solid (shale, sand) and fluid (brine), respectively.

Thermal dispersion has an influence on the total conductivity. The thermal dispersion can be described as a function of the fluid velocity and fluid heat properties. The thermal dispersion tensor which is based on the solute dispersion model [39], reads:

$$\boldsymbol{\lambda} = (\lambda_{eq} + (\alpha_T|\boldsymbol{u}|))\boldsymbol{I} + \rho_f C_f(\alpha_L - \alpha_T)\frac{\boldsymbol{uu}}{|\boldsymbol{u}|} \tag{4}$$

where $|\boldsymbol{u}|$ is the magnitude of the Darcy velocity vector and α_L and α_T are the thermal dispersion coefficients in the longitudinal and transversal direction, respectively.

The pore fluid used in the dynamic model is brine. The brine has a constant specific heat capacity, heat conductivity and salinity (Table 1). The viscosity of the brine varies with temperature (T) and S the salinity of the brine [ppm/10^6] [35] as:

$$\mu = 0.1 + 0.333S_a + (1.65 + 91.9S_a^3)e^{\{-[0.42(S_a^{0.8}-0.17)^2+0.045]T^{0.8}\}} \tag{5}$$

The density of the brine depends on the temperature, the pressure and the salinity (S_a) as:

$$\rho_f = \rho_w + S_a\{0.668 + 0.44S_a + 10^{-6}[300P - 2400PS_a + T(80 + 3T - 3300S_a^3P + 47PS_a)]\} \tag{6}$$

where

$$\rho_w = 1 + 10^{-6}(-80T - 3.3T^2 + 0.00175T^3 + 489P - 2TP + 0.016T^2P - 1.3\times10^{-5}T^3P - 0.333P^2 - 0.002TP^2) \tag{7}$$

For Eqs. (5)–(7), T is in [°C] and P in [MPa] [35].

The yearly energy production by a geothermal doublet can be calculated through Eq. (8).

$$\Delta\dot{E}_i = \dot{m}_i c_p \Delta T_i \tag{8}$$

where $\Delta\dot{E}_i$ (J/year) is the annual thermal energy extracted in the i^{th} year, $\dot{m}_i$ (kg/year) is the total mass production of hot water in the i^{th} year, c_p (J/kg K) is the specific heat of the circulating fluid and ΔT_i (K) is the temperature difference between the produced and injected fluid in the i^{th} year. The total produced energy for n years of production can then be obtained as the summation of the energy provided on overall n years (e.g. [40,41]).

2.2. Heavy oil reservoir (Domain 2)

For the oil reservoir (Domain 2) the energy balance and the continuity (including heat loss rate to overburden and underburden and pressure and temperature dependency of fluid properties) are solved by using a non-isothermal numerical reservoir simulator in a 3D Cartesian domain. It is assumed that the reservoir model is at the depth of 800 m and its initial temperature is estimated to be 37 °C. All the cation concentrations in the reservoir are assumed to be in an equilibrium state with the reservoir rocks. The model contains a vertical injection well and a vertical production well (Fig. 2).

For all scenarios hot water with various temperatures, starting at initial oil reservoir temperature up to 140 °C, are injected through injectors for 20 years. The injection rates are 150–1000 m^3/day with an assumption of no restriction in the bottomhole pressure of the injection well. This implies that there is always enough pressure for production, regardless of the size of the reservoir. It is assumed that water is in the liquid phase and can be supplied continuously without well integrity problems in the case of unconsolidated sandstone during the entire injection period. The oil producer is controlled with the bottomhole pressure of 0.7 MPa (100 Psia) and the target rate is the same as the injection rate value. Heat dissipates into reservoir fluid and rock through hot water injection in the injection well and, hence, oil can be produced through the oil production well due to viscosity reduction.

The energy balance Eq. (9) and the mass balance Eq. (10) employed in the non-isothermal black oil model are explained below. The energy balance equation takes the following form

$$\frac{\partial}{\partial t}\left[\phi_2\sum_{i=o,w}(S_i(\rho_i C_{p,i}T - P_i)) + (1-\phi_2)\rho_r C_{pr}T\right] = -\nabla\cdot\sum_{i=o,w}(\rho_i C_{p,i}\boldsymbol{u}_i)T + \nabla\cdot(\lambda_2\nabla T) \tag{9}$$

where the subscripts o, w and r refer to the oil, the water, and the solid phase (rock) respectively.ϕ_2 is the oil reservoir porosity and λ_2 is the bulk thermal conductivity [W/(mK)], ρ [kg/m^3] and S [–] are the density and saturation of each phase respectively. In Eq. (9), it is implicitly assumed that local equilibrium is established [42]. Mass conservation is represented by

$$\frac{\partial}{\partial t}\left[\phi_2\sum_{i=o,w}(S_i\rho_i)\right] + \nabla\cdot\sum_{i=o,w}(\rho_i\boldsymbol{u}_i) - Q^* = 0 \tag{10}$$

where the specific volumetric velocity $\boldsymbol{u}_i$ is given by Darcy's law, $\boldsymbol{u}_i = -kk_{ri}/\mu_i\nabla P_i$, where μ_i is viscosity of each phase (oil/water) and Q^* is source/sink respectively. Here the relative permeability data (k_{ri}), derived from the Brook and Corey correlation, are utilised based on the following parameters: $S_{wi} = 0.17$, $S_{orw} = 0.05$, $S_{org} = 0.1$, $S_{gc} = 0$, $k_{roiw} = 0.4$, $k_{rwro} = 0.4$, $k_{rwro} = 0.1$, $k_{rgro} = 0.2$ and $S_{wir} = 0.17$. Note that the effects of temperature [43] on relative permeability are not considered here.

Viscosity and density are important physical properties of crude oil. However, no practical theory exists for the calculation of these properties for heavy oil at elevated temperatures. In this study, heavy oil viscosity was adopted as a function of API and temperature. The predicted values of the viscosity are used in the next step to develop the fluid model. The oil viscosity and oil density are 850 cp 15° API at the initial reservoir condition respectively [31]. Here, a correlation for prediction of the viscosity of heavy oil as a function of temperature and the oil API is developed [44]. Similar to Bahadori and Vuthaluru [45] and Bahadori [46,47] the identical methodology is applied to develop the correlation. Eq. (11) represents the proposed correlation for the viscosity of heavy oil as a function of temperature and the API:

$$\ln(\gamma) = a_1 + \frac{a_2}{API} + \frac{a_3}{(API)^2} + \frac{a_4}{(API)^3} \tag{11}$$

where for i = 1, 2, 3, 4, the parameter a_i is equal to

$A_i + B_i$ T+ $C_i T^2 + D_i T^3$. The fitted constant coefficients calculated by the least square method are listed in Fig. 3a. Note that in Eq. (11) the temperature is in °C and the kinematic viscosity measured in cSt, γ, can be converted to dynamic viscosity in cp, μ, by multiplying by oil specific gravity [44]. Fig. 3a shows the regression result and a comparison between the experimental data with calculated viscosities at different temperatures in °C.

2.3. Models validation

In this section before presenting results, which document the impact of various effective parameters such as injection temperature/rate on heavy oil recovery, the numerical uncertainties for model convergence evaluation are considered. In general, discretization errors are the dominant sources of numerical errors in computational simulations (e.g., [48]). In order to minimize numerical uncertainties, such as numerical dissipation, it is essential to choose a proper grid discretization. This provides some assurance that potential inaccuracies associated with discretization are relatively small. The base case is modelled using different grid sizes, from coarse to fine. The size of the grid cells is gradually decreased until there is no significant difference in the numerical results between two successive mesh densities. For the geothermal model (Domain 1), discretised by 3D tetrahedral and hexahedral finite elements (Fig. 2c), a maximum finite element mesh size of 20 m × 20 m × 2.5 m is chosen based on study of Saeid et al. [49]. The minimum finite element mesh size is 0.5 m. Saeid et al. [49] analysed the discretisation error for a similar dynamic model and found that the chosen mesh size results in a negligible discretisation error for the fluid and heat transfer simulations for the range of studied parameters. In this study, the relative and absolute error tolerances for flow and heat transport simulations are set to 10^{-5} and 10^{-6}, respectively. Similarly, the results for the oil reservoir model (Domain 2) indicate that a grid cell with an average grid size of 5 m × 5 m × 5 m (100, 40 grid cells in x, y and 6 in z directions respectively) is sufficient (Fig. 3b).

3. Results

In this study several scenarios are examined to understand the degree by which different reservoir parameters affect heavy oil production. The parameters selected for the sensitivity analysis with their corresponding minimum and maximum values are listed in Table 3.

3.1. Geothermal reservoir (Domain 1)

For the geothermal reservoir (Domain 1), the transient water temperature at the production well is calculated in order to estimate the life time of the geothermal doublet. The life time of the geothermal doublet is defined as the time when the production fluid temperature drops below the minimal production temperature (here 90 °C). In this study the temperature losses in the wells are neglected. Saeid et al. [49], by simulation of flow and heat transfer in the reservoirs and in the wells surrounded with the rocks, illustrated that the temperature losses in the wells have negligible effect - in the long term - on the temperature of the production fluid of a geothermal system due to the fast flow condition in the wells.

Fig. 4 illustrates the contribution of the injection rates on the production well performance of the geothermal doublet. These results show that although a low injection rate enhances the lifetime (Fig. 4a) it decreases the produced energy (Fig. 4b). There is a significant reduction in the lifetime of the system when the discharge increases from 2400 m^3/day to 6000 m^3/day [41]. For higher injection rate values, this effect becomes less significant which is in accordance with the findings of Saeid et al. [49]. Based on this analysis, the geothermal aquifer can serve as a long term source for hot water injection into the oil reservoir during the enhanced thermal heavy oil recovery project.

3.2. Oil reservoir (Domain 2)

3.2.1. Effect of wellbore distance

The optimum distance between the producer and injector can be determined based on geology, ease of drilling and operation, and maximum production operation conditions such as flow rates. In order to investigate the impact of wellbore distance on oil recovery five different well spacing scenarios have been considered: 100, 200, 300, 400 and 500 m, while all other parameters are kept as for the base case. Fig. 5 shows the effect of wellbore distance on ΔTOP when various injection rates (150–1000 m^3/day) are applied. ΔTOP indicates the total/cumulative oil production (TOP) difference (oil recovery) between conventional water flooding (the injected water temperature similar to that of the oil reservoir) and hot water flooding.

As illustrated in Fig. 5, scenarios with increased wellbore distance decrease the ΔTOP for short time injection (less than 10 years). Also for short time injection, the highest oil recovery is observed when the injection rate is highest and wellbore distance is lowest. By contrast, as shown in Fig. 5f, for injection periods of more than 10 years (point A) the wellbore distance of 200 m gives higher oil recovery, related to the higher amount of original oil in place (OOIP) between production and injection wells. Furthermore, by continuing the injection period approximately for 20 years, the oil recovery for the scenario with 100 m wellbore distance reaches that of the system with a 300 m wellbore distance. However, at this time, the corresponding oil recovery (point B) is still less than that of the system with 200 m wellbore distance.

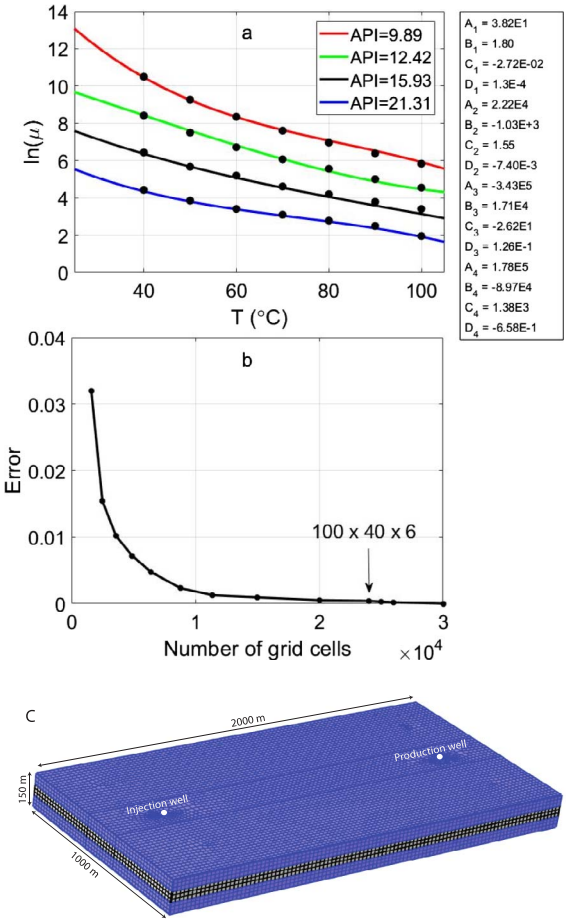

Fig. 3. (a) Comparison between calculated viscosity (solid lines) after regression analysis with the experimental data (symbols) [31]. (b) Grid sensitivity analysis for oil reservoir (Domain 2). (c) The mesh utilised for Domain 1 with the model size of 2000 m × 1000 m × 150 m.

Table 3
The range of the parameters used for the sensitivity analysis are based on the data from the deep geothermal projects in the Netherlands (http://nlog.nl/geothermie).

Geothermal reservoir (Domain 1)	
Reservoir porosity (–)	0.1 – 0.4
Reservoir permeability (mD)	250–1250
Injection rate (m^3/h)	100–250
Oil reservoir (Domain 2)	
Reservoir porosity (–)	0.1–0.4
Reservoir permeability (mD)	300–1250
Injection rate (m^3/day)	150–1000
Injection temperature (°C)	60–140
Wellbore spacing (m)	100–500

3.2.2. Effect of injection temperature and rate

Although injection temperatures and rates have direct effects on the oil recovery, these effects strongly depend on the operational conditions (e.g., bottomhole pressure). To quantify such effects several scenarios are studied. Fig. 6 displays predicted total oil production curves for both, various injection temperatures and rates. The curves depict the behaviour for 20 years of continuous injection. Fig. 6a shows that the oil recovery is slightly affected by the temperature of the hot water injection when injection rate remains low (150 m^3/day). By contrast, at higher injection rates the injection temperature has a significant influence on the oil production (Fig. 6d–f).

Apart from these assessments, the effects of non-uniform injection and production rates on oil production are further examined. As shown in Fig. 7, the oil recovery has a higher sensitivity to the injection temperature when the injection rate is less than production rate. This is related to the lower water cut in the production well.

The simulation results show that the oil recovery is rather insensitive to increasing of the injection temperature at injection rate higher than the production rate. Moreover, increasing the injection rate beyond the production rate reduces the oil recovery improvement considerably.

3.2.3. Effect of oil reservoir porosity and permeability

Five different average oil reservoir porosities: 10%, 18%, 25%, 30%, and 40% are considered to compare the total oil recovery between the conventional water flooding (37 °C) and the hot water flooding (100 °C). Fig. 8 shows the ΔTOP (i.e. the total/cumulative oil production difference between conventional water flooding and hot water flooding) curves for these scenarios with different injection rates of 150, 250, 500, 750 and 1000 m^3/day. The results show that increasing the porosity leads to a higher ΔTOP . For the scenarios with high injection rates the oil reservoir porosity has a significant effect on the oil recovery.

The impact of reservoir permeability on ΔTOP is shown for models with a hot water flooding (100 °C). In fact, ΔTOP seems to slightly decrease for increasing permeabilities within the range investigated. While oil recovery is increased with increasing injection rate the permeability increase has an adverse effect on ΔTOP.

3.2.4. Consumed energy for the thermal oil recovery

As mentioned before the hot water (heat) can be provided from a geothermal doublet. Figs. 9–11 indicate the cumulative oil production (ΔTOP) versus the cumulative injected (hot water) energy in the oil reservoir domain. The cumulative injected energy (E_{inj}) with respect to the initial oil reservoir temperature (T_{init}) in the oil reservoir domain is calculated through

$$E_{inj} = \sum_{i=1}^{n} Q_i \Delta t \rho_f Cp_f (T_{inj} - T_{init}) \quad (12)$$

where Δt is the time step [day], n is the number of time steps, Q_i is the hot water injection rate and T_{inj} is the injection temperature. Fig. 9 shows the model with the wellbore distance of 200 m is the most effective one for oil production. The highest ΔTOP and ΔRF (i.e. the recovery factor, *RF*, difference between conventional water flooding and hot water flooding) are displayed for E_{inj} in the range between 300 and 1000 GWh. Point *A* in this Figure indicates that the oil productions (ΔTOP) for 100 m and 200 m wellbore distance are identical at E_{inj} = 250 GWh. However, for E_{inj} less than 250 GWh (point *A*) the 100 m distance gives the highest oil production.

The hot water injection is continued for a long time to study the produced oil values for different wellbore distances. As shown in Fig. 9 the ΔTOP for 100 m is less affected by the used energy and only increases slightly with higher energy input. For larger well distances, however, the increase of total production is greater with increasing energy input. At points *C* and *D* in Fig. 9 the amount of the ΔTOP and E_{inj} for 100 m well spacing are equivalent to those for 400 m and 500 m well spacing, respectively.

Moreover, our results show almost a linear relation between the total oil production enhancement and E_{inj} for 400 m and 500 m wellbore distances. With continuing energy injection over time from 5 to 1000 GWh, ΔTOP increases from 1.8 to 4.2 × 10^4 m^3 when the wellbore distance is 500 m. However, at 1000 GWh cumulative energy injection, the highest value of the oil recovery is observed for 200 m wellbores distance.

To address the effect of different injection temperatures and rates on the oil production and E_{inj} two scenarios are studied. Fig. 10a and b depicts the effect of different injection rates and temperature on the oil recovery over the consumed energy. For higher injected temperature the oil recovery curves are least sensitive to the injection temperature changes at constant injection rate (Fig. 10a). In contrast such a curve is most sensitive to different injection rates at constant injection temperature (Fig. 10b). For low E_{inj} values (37.5 GWh) the injection rates 250 and 500 m^3/day give same oil production amount about 7.5 × 10^3 m^3 (Fig. 10d). Such behaviour can also be observed for different injection temperatures in Fig. 10d. Note that this happens at different time affecting the economy of the project.

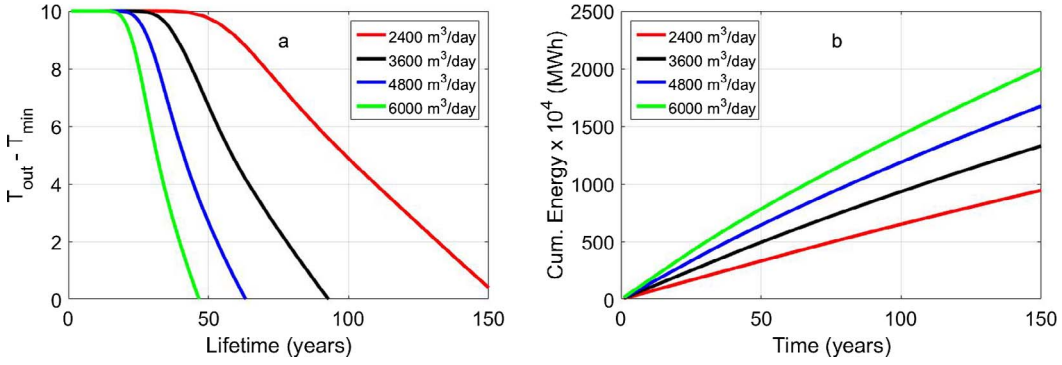

Fig. 4. Geothermal production well performance for four different injection rates (m^3/day).

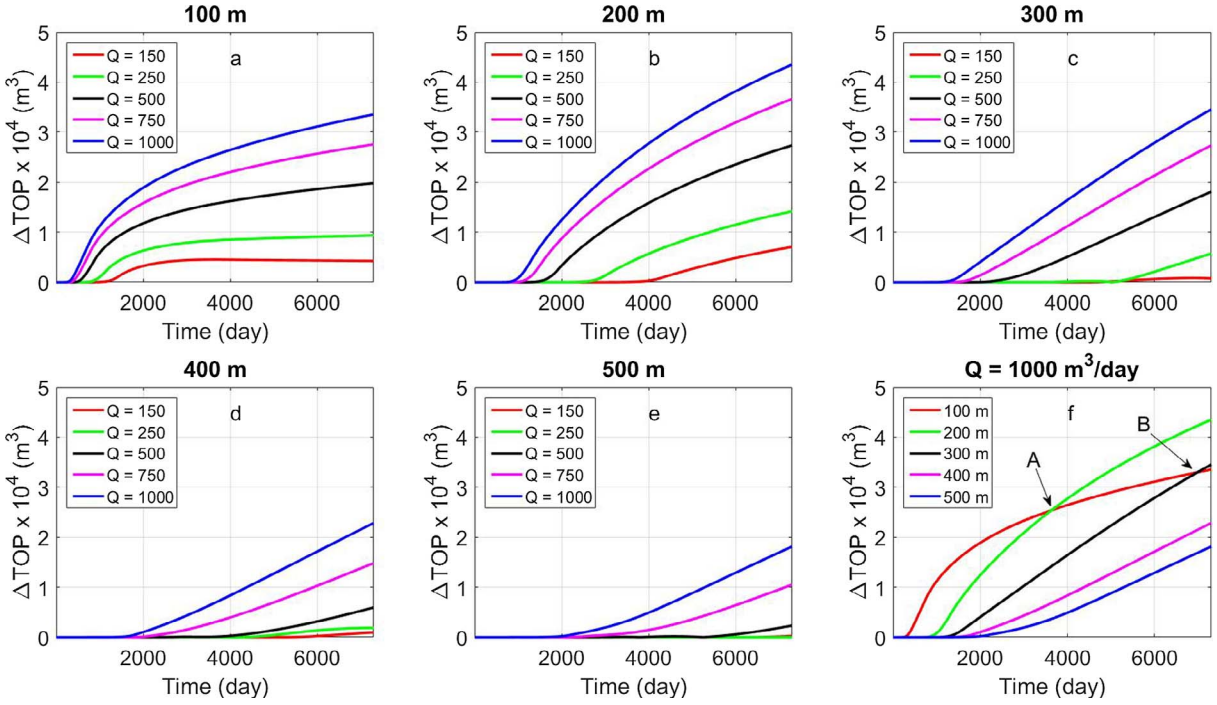

Fig. 5. Effect of the wellbore distance on ΔTOP for various injection rate, Q, (m^3/day) when $\phi = 0.18$, $k = 496$ mD and 100 °C injection temperature.

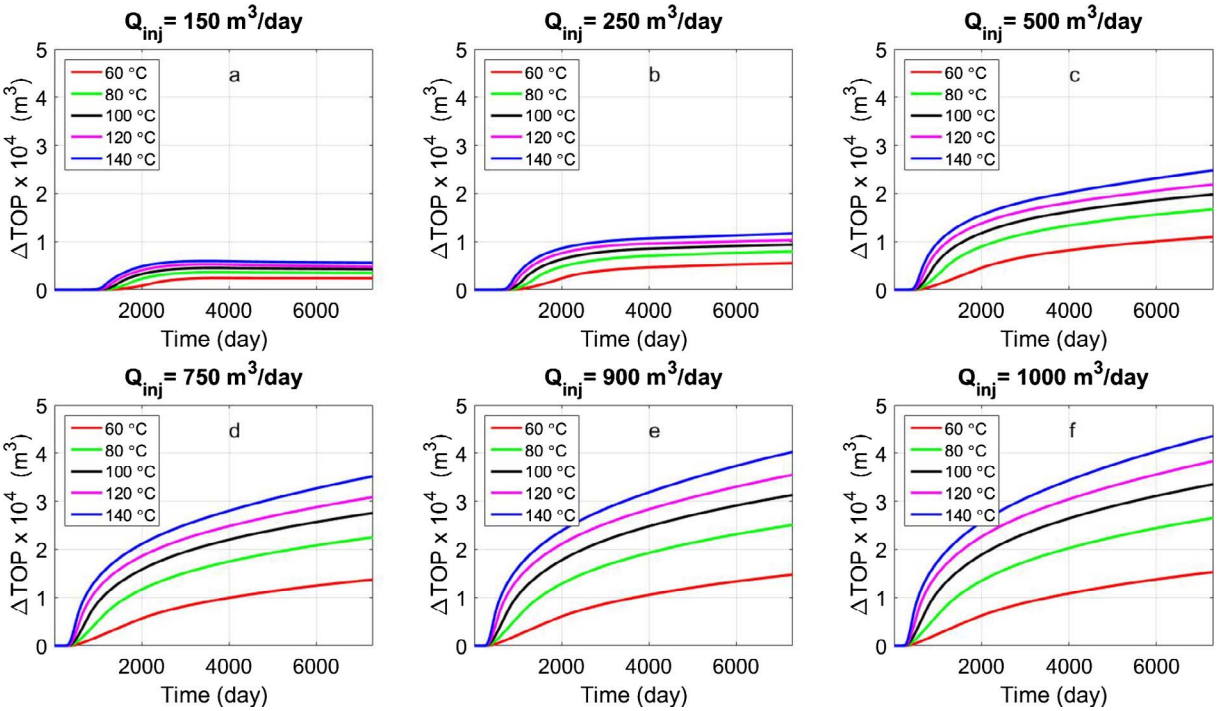

Fig. 6. The effect of the injection rate and temperature on total oil production (ΔTOP) for 100 m wellbore distance, $\phi = 0.18$ and $k = 496$ mD.

In Fig. 11, the effects of porosity and permeability on the oil recovery versus E_{inj} are displayed analogous to Figs. 6–8. The effect of porosity is strong, with a general increase of total oil recovery the higher the porosity value is. For permeability, the effect is much less pronounced. In general, higher permeabilities have a slightly negative effect on total oil production, especially with increasing energy input.

Fig. 12 demonstrates the oil production well performance in the oil reservoir domain. The temperature profile in the production well progressively increases up to ~90 °C after approximately 1000 days (Fig. 12b) when the injection rate in the oil reservoir is more than 500 m^3/day. Also as shown in Fig. 12d and e while values of the water production temperature are sensitive to the injection rate/temperature and wellbore distance, they are almost unaffected by the porosity and permeability variations.

It is assumed, in the onset of the hot water flooding, surface water with temperature of 10 °C (T_s) and with similar thermal properties of the formation water can be utilised until enough water for reinjection is produced from the oil reservoir (Fig. 12a). As shown in Fig. 12b, at the later stage of oil recovery, the produced water temperature increases and the temperature drop (the temperature difference between the

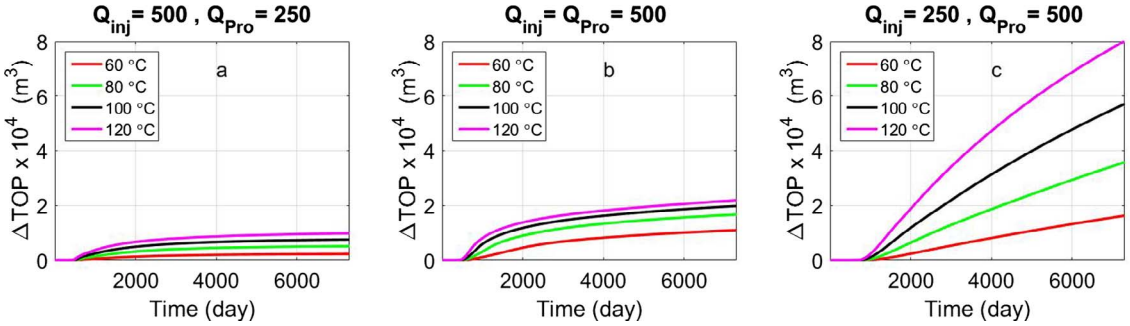

Fig. 7. ΔTOP variation for different injection temperature and rate, Q, (m^3/day) for 100 m well distance, $\phi = 0.18$, $k = 496$ mD, L = 100 m. Injection rate is (a) larger, (b) equal and (c) less than the production rate, respectively.

injection and the production wells) is about 10 °C for injection rate more than 500 m^3/day. This implies that less energy is required for heating of the injection water for the oil reservoir. This behaviour is a positive factor to compensate part of the energy input in the oil reservoir.

When the thermal front reaches to the production well the oil production enhancement occurs and hence the temperature profile in the production well raises from initial reservoir temperature to approximately injection temperature. Thus the net cumulative energy consumption for the oil reservoir can be defined as

$$E_n = \sum_{i=1}^{j} \Delta t_j \rho_f Cp_f (Q_{inj}^w T_{inj} - (Q_{inj}^w - Q_{pro}^w) T_s - Q_{pro}^w T_{pro}) \quad (13)$$

where Q_{inj}^w and Q_{pro}^w are water injection and production rate (m^3/day) of the oil reservoir and j is the number of injection years. T_{inj} and T_{pro} are water temperature in the injection and production wells in the oil reservoir respectively.

Figs. 13 and 14 show the total cumulative oil production versus E_n. From Fig. 13 a number of distinct features can be observed. First energy required to produce oil for 500 m wellbore distance is about 2 time larger than that of the 300 m wellbore distance at end of 40 years. Secondly, at a given net cumulative energy consumption (E_n = 26 GWh) the oil productions and hence the oil recovery (that is ratio of the oil production over the OOIP) for 100 m wellbore distance is equivalent to those for 200 m. Such behaviour is also exhibited for 300 m, 400 m and 500 m wellbore spacing. Results of this study demonstrate that the optimum wellbore distance considering the E_n larger than 200 GWh and oil recovery is 200 m.

From Fig. 14b it is evident that by growing the consumed energy more than 40 GWh the optimum amount of oil production is exhibited for the 1000 m^3/day injection rate. Also for injection rates less than 500 m^3/day due to consumed energy enhancement (after 35 GWh) the oil production will not reach a significant value and becomes constant. For the energy consumption more than about 50 GWh, the result for 100 °C injection temperature is similar to that inferred for injection temperature of 120 °C and no significant oil recovery improvement is observed for T_{inj} larger than 100 °C (Fig. 14b). It is important to highlight that if only recovery is considered the higher injection temperature results in higher ΔTOP (Fig. 6c) and if the net cumulative energy consumption is also considered ΔTOP is rather insensitive to the injection temperature higher than 100 °C for a given energy consumption of more than 50 GWh.

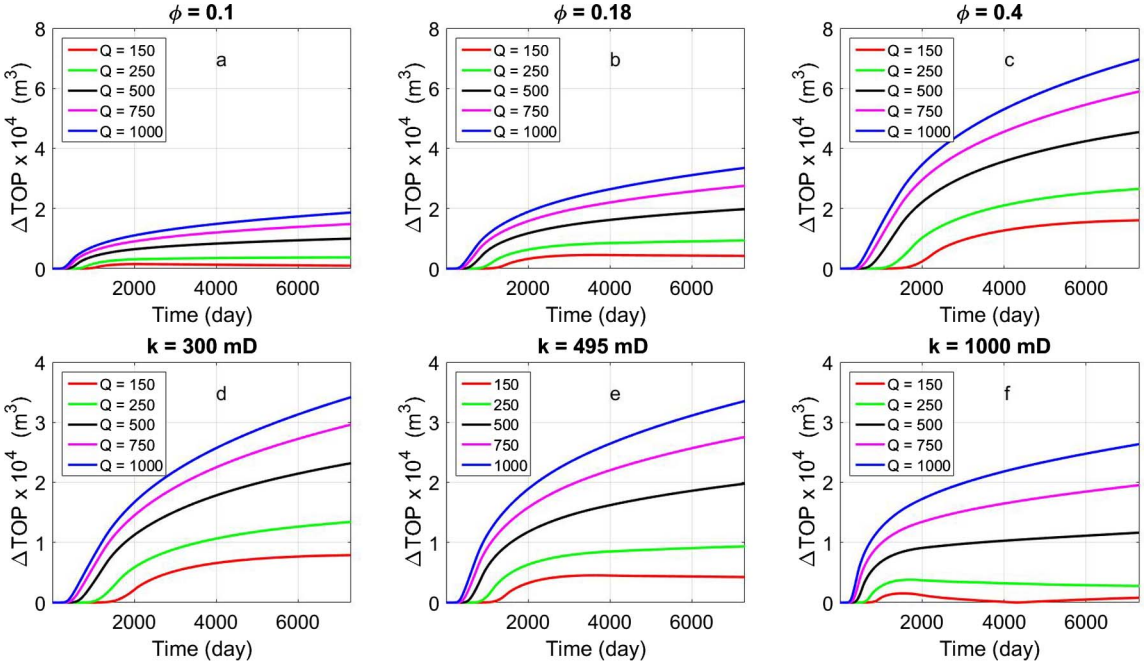

Fig. 8. ΔTOP versus time for various reservoir porosity, permeabilities and injection rate, Q, (m^3/day) for a system with 100 m well distance and 100 °C injection temperature for (a–c) $k = 496$ mD and (d–f) $\phi = 0.18$.

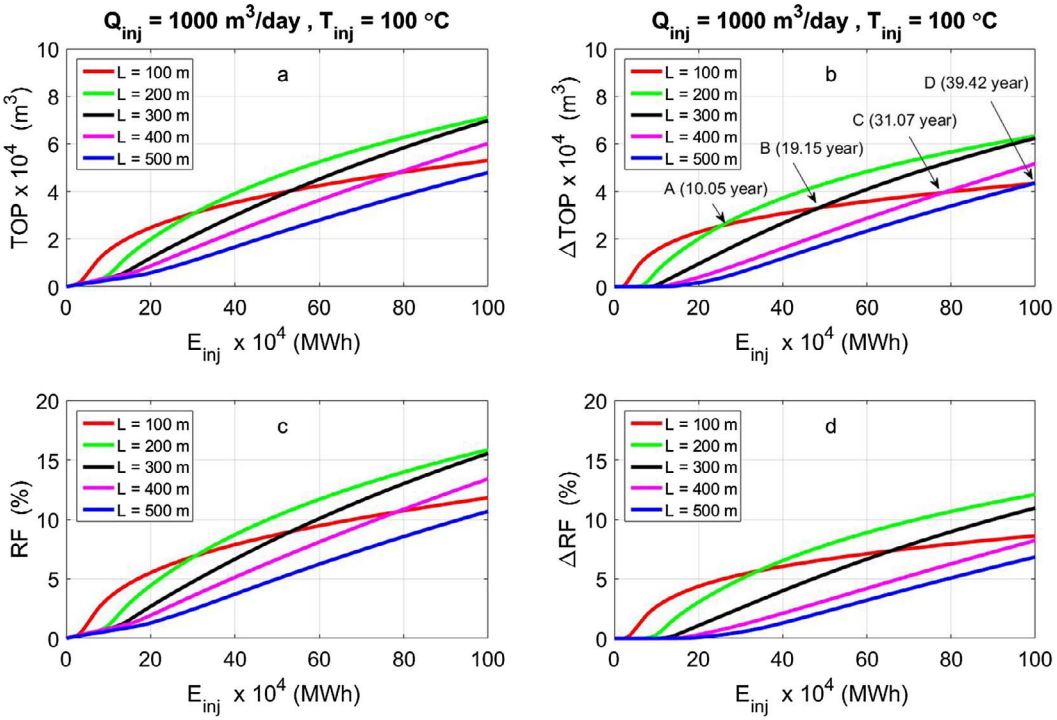

Fig. 9. (a and b) ΔTOP and TOP, (c and d) $\Delta RF = \Delta TOP/OOIP$ and $RF = TOP/OOIP$ versus E_{inj} in the oil reservoir for various wellbore distances for $\phi = 0.18$ and $k = 496$ m. (OOIP = 44.874×10^4 m^3).

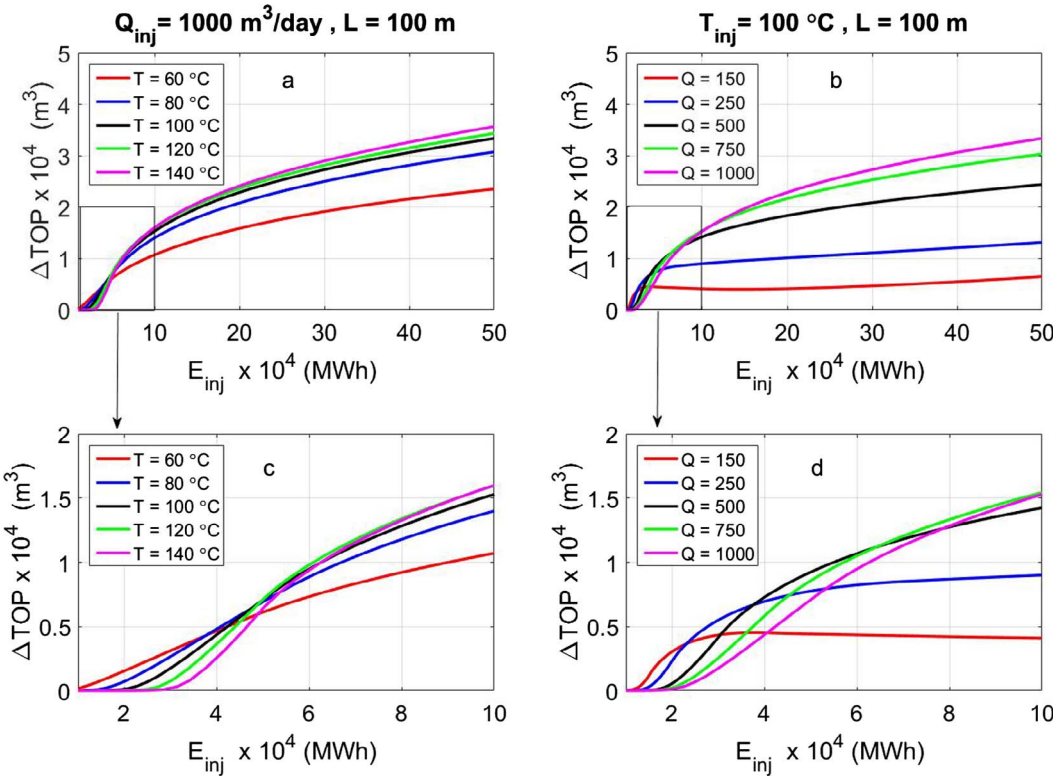

Fig. 10. ΔTOP and E_{inj} in the oil reservoir for various injection rates, Q, (m^3/day) and temperatures for a reservoir with $\phi = 0.18$ and $k = 496$ mD.

4. Discussion

4.1. Geothermal reservoir (Domain 1)

For the geothermal reservoir, the focus is on energy harvesting from a well doublet. The two parameters used here are injection rate and initial geothermal reservoir temperature of 100 °C in order to provide required energy for heavy oil production. The influences of other parameters such as porosity, permeability, reservoir heterogeneity and fractures on geothermal doublet performance have been explored in detail by previous studies (e.g., [20,40,50,51]). Saeid et al. [40] investigated various factors influencing non-isothermal flow in

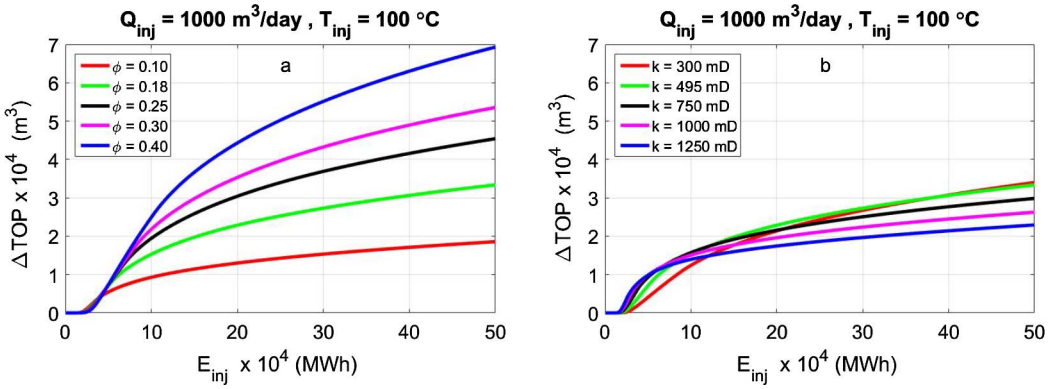

Fig. 11. Δ*TOP* versus E_{inj} in the oil reservoir for various porosity and permeability when wellbore spacing is 100 m.

geothermal reservoirs such as porosity, geothermal fluid salinity, flow rate, well spacing and injection temperature. They suggested a relation expressing life time of the geothermal reservoirs as a function of the studied parameters. Similarly, Crooijmans et al. [20] considered the influence of the facies distribution for heterogeneous media on geothermal doublet performance in the Netherlands. The current study addresses cumulative energy production from a geothermal doublet with various injection rates (Fig. 4).

The results show that the cumulative energy harvesting over 20 years from a geothermal doublet for injection rate 4800 (m^3/day), is 2660 GWh which is much bigger than the energy required for enhanced thermal oil recovery for a single injection and production well in the Moerkapelle field. This provides enough energy for additional purposes or for heating up the water for many injection wells utilising hot water flooding scheme for the oil reservoir depending on their injection rates.

4.2. Oil reservoir (Domain 2)

4.2.1. Wellbore spacing

The key objective in the hot waterflooding process is to achieve a high temperature distribution around the oil production wellbore. For long distance between the injection and production wells it takes longer for the heat plume to arrive at the producer such that the oil viscosity reduction initially just happens near the injector. In that case no significant oil saturation alteration in the reservoir and near the producer is observed. As a result, efforts are ongoing to improve the temperature distribution and allow the heat to reach the producing wells, enabling production of oil with reduced viscosity. This may be achieved by either reducing the distance between injection and production wells or longer hot water injection time.

The well spacing is thus a critical parameter in an economic study on thermal EOR. While smaller well spacing accelerates the time needed for a viscosity reduction and enhanced production, a larger well spacing covers a higher amount of original oil in place (OOIP). Our results show that the 200 m wellbore distance gives the optimum value of oil recovery (Fig. 11), related to the higher amount of original oil in place (OOIP) between production and injection wells (drainage area) compared to smaller well spacing and faster production. This is in accordance with the results of Cheung et al. [52], Zhao et al. [53] and Verney [54], illustrating that the optimum well spacing in hot waterflooding or steam flooding is approximately between 80 and 250 m when the project economics are taken into consideration. Although

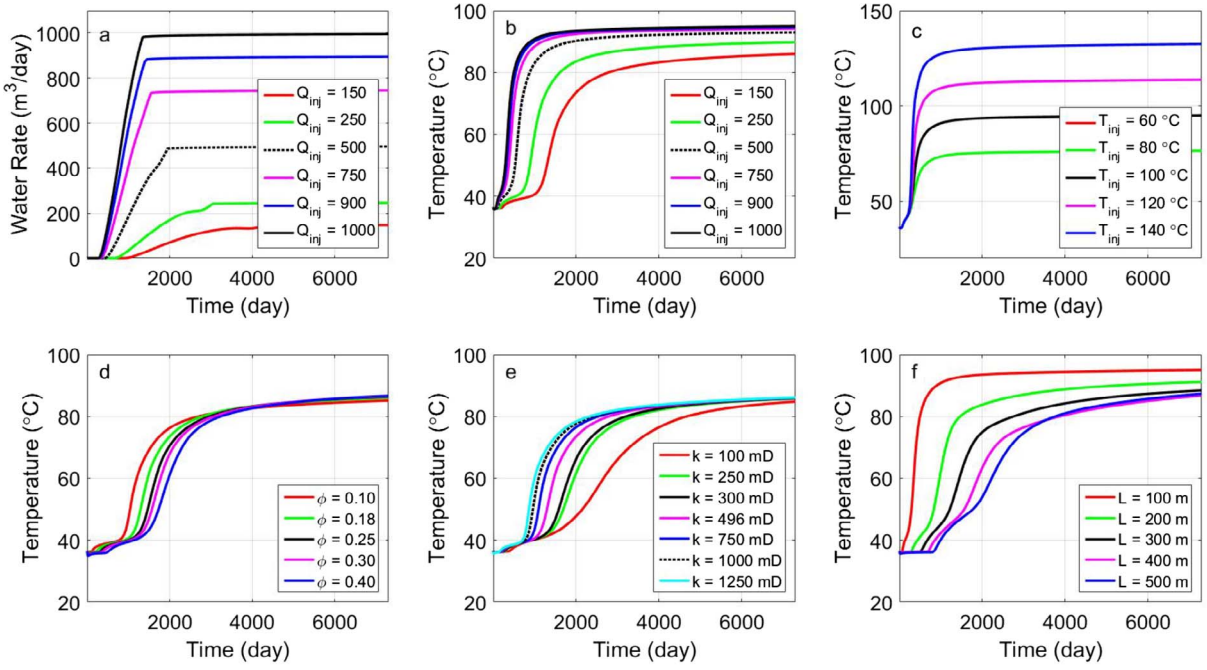

Fig. 12. Sensitivity analysis for oil production well performance a case with T_{inj} = 100, well distance of 100 m, T_{inj} = 100 °C, k = 495 mD, and porosity of 0.18 for (a) produced water rates induced by various injection rates; and temperature profile for various (b) injection rates, (c) injection temperatures with Q_{inj} = 150 m^3/day, d) porosities with Q_{inj} = 150 m^3/day, (e) permeabilities with Q_{inj} = 150 m^3/day and (f) wellbore distances in oil reservoir domain with Q_{inj} = 1000 m^3/day.

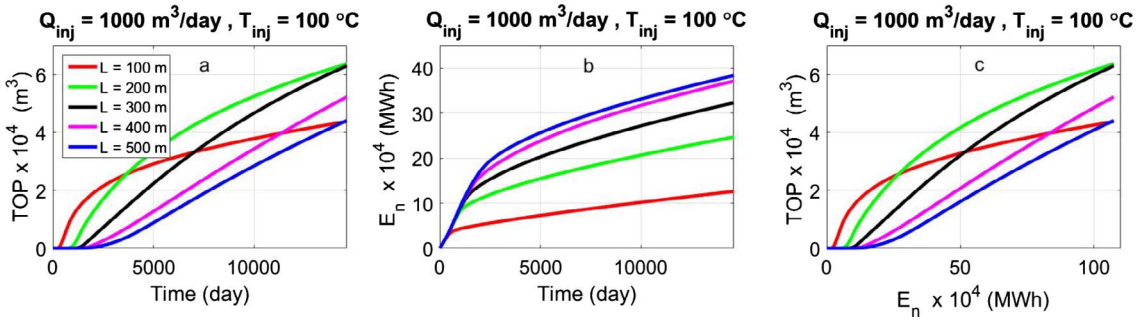

Fig. 13. (a) *TOP*, (b) the cumulative net consumed energy (E_n) vs. injection time and (c) *TOP* vs. cumulative net consumed energy (E_n) in the oil reservoir for various wellbore spacing in the reservoir with $\phi = 0.18$ and $k = 496$ mD.

short distance between the injector and producers leads to favourable oil recovery, well space reduction is not the best way because well drilling costs and also early high water cut in the producers are not favourable [55]. In contrast when the wellbore spacing increases, the injection period dramatically advances, as a major issue, to carry the heat toward the oil production well. However, the optimum wellbore spacing depends likely on oil viscosity. For oil with high viscosity, shorter wellbore spacing would be required compared to when the reservoir contains oil with low viscosity. This dependency, however, has not been investigated in detail yet and is subject to further studies.

4.2.2. Impact of reservoir properties

This study illustrates that higher permeability causes early water cut for hot water flooding in the reservoir resulting in the oil recovery reduction. However, the opposite behaviour is observed for increasing porosity. Fig. 15 shows that porosity and permeability variation influence the shape and the size of the heat plume. For example, the heat plumes have a narrower teardrop shape in the reservoir with a smaller porosity. In contrast, the heat plume expands in a more symmetrical manner for the reservoir with a lower permeability. The porosity and permeability variations forms the pressure distribution and the shape of the heat plumes.

Here only the effect of different porosity and permeability values on the performance of the energy production is addressed. The impact of other parameters such as reservoir heterogeneity, thermal properties of the reservoir rock and reservoir dimensions (e.g., thickness) need further demonstration.

4.2.3. Thermal energy consumption in the oil reservoir domain

Higher injection rates and injection temperature result in better oil sweep in the reservoir at a shorter time despite an earlier water breakthrough. This means that at high injection rate the heat could be transferred faster towards the production well leading to higher oil production. The improved oil recovery for some of the scenarios can be the same for a given cumulative energy consumption. This however happens at different time depending on the injection rate and the well spacing.

Very high injection temperature (e.g. 140 °C) results in better oil recovery in a shorter injection time in spite of the fact that an additional source of energy is required to heat up the water for injection beyond the 100 °C from the geothermal producer. This is true if only the net cumulative energy consumption is not a concern in the analysis. It is noteworthy to mention, such result is acceptable when the amount of the injection and production rates are the same. However, as mentioned earlier, the oil recovery is rather insensitive to increasing of the injection temperature at injection rate higher than the production rate. In this study the efficiency of heat exchangers as well as the economic analysis are not considered. Future work should address these for further improvement of the results.

4.2.4. Synergy of geothermal and heavy oil exploitation

The focus of this study is to examine a strategy for the integration of geothermal energy with heavy oil production from a stranded oil field exploitation. It is also important to find how many oil wells can be realised using a single geothermal doublet. Fig. 16 illustrates what fraction of the produced geothermal energy is required for the improved oil production. For example, for consuming about 10% of extracted energy from a geothermal doublet, 2.68×10^4 m^3 of oil could be produced which is about 6% of the OOIP (4.48×10^5 m^3) of the oil reservoir with the wellbore distance of 200 m. Therefore, the geothermal doublet could provide enough thermal energy for hot waterflooding for more than ten doublets in the oil reservoir considering that less geothermal energy is needed for heating up the injection water once the warm water has reached the production wells.

It is evident that the geothermal reservoir is able to provide the hot water required for the heating of the water for flooding of the oil reservoir as well as for the heating of greenhouses or other buildings nearby. Less than 7 percent of geothermal energy can produce

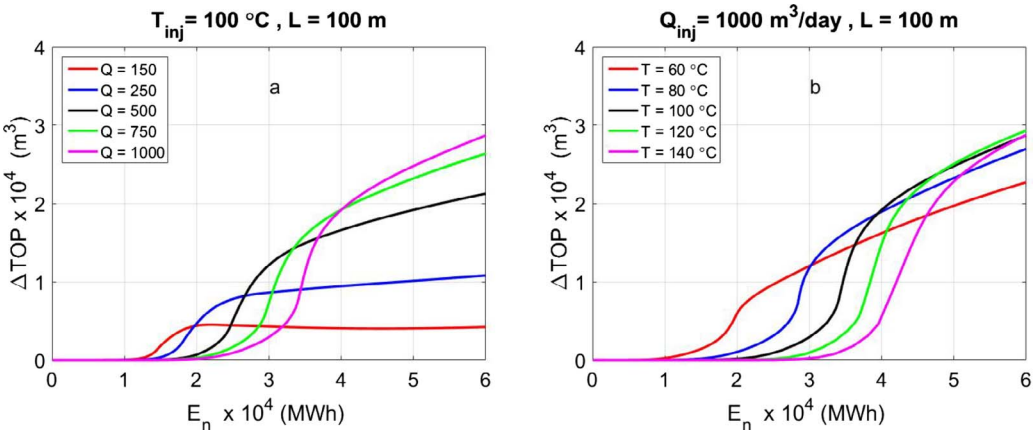

Fig. 14. Δ*TOP* versus the cumulative net consumed energy (E_n) in the oil reservoir for (a and b) various injection rates (m^3/day) and temperatures when $\phi = 0.18$, $k = 496$ mD and 100 m wellbore spacing.

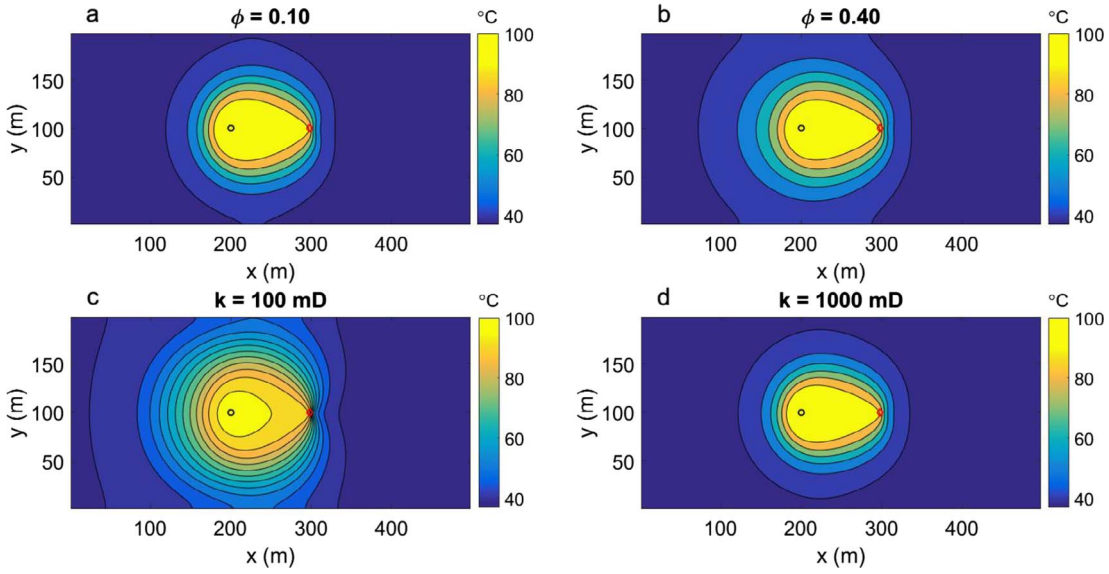

Fig. 15. Plane view of the heat plume shape for different (a and b) porosity and (c and d) permeability values for a system with the injection rate of 250 m^3/day and injection temperature of 100 °C after 20 years of hot water flooding (small black and red circles are the location of the injection and production wells, respectively). (For interpretation of the references to color in this figure legend, the reader is referred to the web version of this article.)

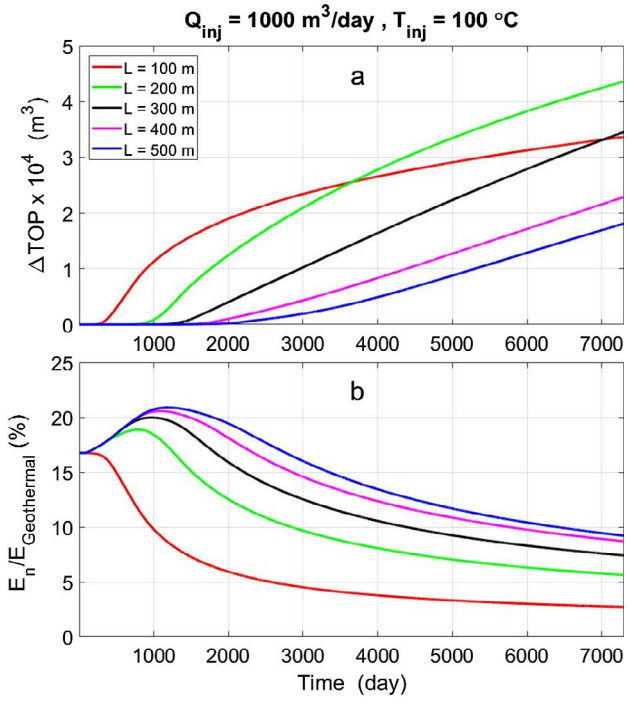

Fig. 16. (a) ΔTOP and (b) the ration of consumed net cumulative energy per cumulative geothermal energy for various wellbore spacing of a reservoir with $\phi = 0.18$ and $k = 496$ mD for 20 years of hot water flooding.

4.48×10^4 m^3 of oil (Fig. 16b) after 20 years when the wellbore distance is 200 m. Such amount of oil produced could make the geothermal business case independent of subsidies and may be a viable option to reduce the overall project cost.

4.3. Feasibility analysis

Geothermal projects, as renewable energy projects, are not economically attractive under a business as usual situation at the current state of development; for this reason subsidies are provided by energy and environmental authorities in order to increase the interest in such projects. The main hypothesis in this feasibility analysis is that the synergy between a geothermal and an EOR project would make the first subsidy-independent, therefore subsidies where not taken into account despite the fact that they could be received (making the project more interesting from an investor point of view).

The feasibility analysis is developed under a pre-royalty-pre-tax framework at this study (Fig. 17); the main reasons for this decision are legal. As there are no similar projects in the Netherlands it is not known how they would be taxed by the authorities; as well as how is going to be decided which equipment belongs to each side of the project (Geothermal-EOR for heavy oil). Similar to Aramburo Velez [56], the oil price used is 50 USD/STB (~45.5 Euro/STB), heat price 0.012 Euro/kWh [57] and the discount rate is 8%. The Investment and Operational costs (CAPEX and OPEX) and the price of the heat used in the Economics of the Geothermal Project are based on a price per kilowatt (kW) output of heat as reported by ECN [57]. Table 4 compiles the information regarding the calculation of the NPV for the geothermal project and EOR project. It should be mentioned that, however, the cost associated with the wellbore distance reductions are not taken into NPV account.

The results show the synergy between geothermal and EOR of 200 m well spacing may reduce the required subsidy for a single doublet geothermal project up to 50%. This feasibility is also confirmed by study of Aramburo Velez [56] who studied utilisation of geothermal heat for thermal EOR in the Moerkapelle oil reservoir with horizontal wells. He pointed out that for scaling up the process and considering more than one doublet in a homogeneous oil reservoir, the extra oil and heat production obtained could pay for the project without requiring any subsidy [56]. The NPV analyses for different injection temperature show that, at higher injection temperature (e.g. 140 °C) beyond the 100 °C obtained from the geothermal producer the required subsidy for a single doublet geothermal project reduces up to ~75% in spite of the fact that an additional source of energy is required to heat up the water for injection (Fig. 17b). The positive effect on the NPV is partly due to the fact that injection of 140 °C results in higher temperature of the water produced in the oil production well at the later time which reduces the cost of the heating of the injection water. This however requires more detailed analysis by considering the actual cost of different sources of energy for heating the injection water for the oil reservoir.

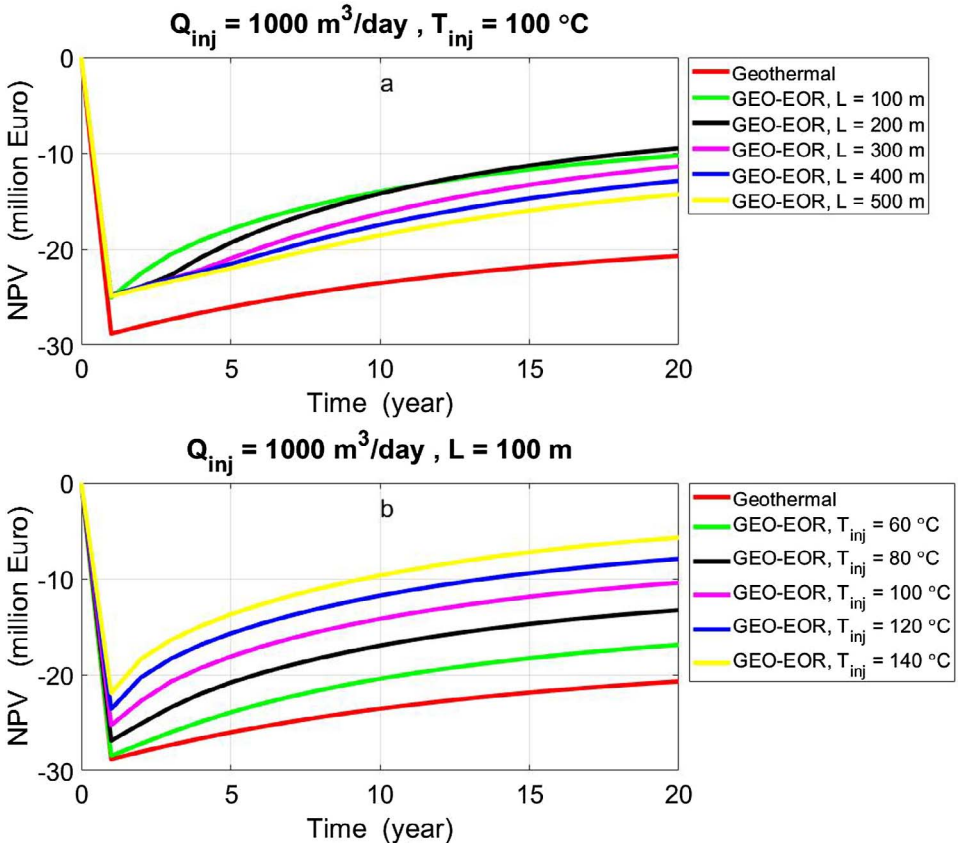

Fig. 17. Net Present Values of the synergy project for various (a) wellbore spacing and (b) injection temperature of the oil reservoir with $\phi = 0.18$ and $k = 496$ mD for 20 years of hot water flooding.

Table 4
Variables used in the NPV calculation of the Geothermal and EOR sides of the synergy (after ECN [57]). CAPEX and fixed OPEX are calculated with the capacity of the installations, while variable OPEX is calculated with the actual output of the system [56].

Item	Value	Unites
Geothermal side		
CAPEX	1622	Euro/kW (capacity)
Fixed OPEX	59	Euro/kW/year (capacity)
Variable OPEX	0.008	Euro/kWh/year (output)
EOR side		
CAPEX	1,440,000 €	Total for two wells drilling, pump energy and also well stimulation[a]
Fixed OPEX	3%	of cumulative CAPEX/year
Variable OPEX	11.45	Euro/sm3 (oil)
Oil Evacuation costs	11.45	Euro/sm3 (oil)

[a] The CAPEX is developed based on Van Wees et al. [58] method.

5. Conclusion

In order to assess the synergy potential of the oil and the geothermal production examining different thermally enhanced oil recovery strategies by utilizing the combination of the two models: (a) a geothermal aquifer (Domain 1) and (b) an oil reservoir (Domain 2) is proposed. To this end, a finite element non-isothermal flow model for geothermal doublet and a non-isothermal flow transport modelling for the oil reservoir are utilised to handle the combined heat and multiphase flow simulations, respectively. The roles of injection temperature and flow rate, reservoir porosity, reservoir permeability and well spacing on the improved heavy oil recovery are addressed. On the basis of a multi parameter analysis the following can be concluded:

- For a long distance between the injection and production wells and short time period injection the high temperature profile does not arrive at the producer and hence the oil viscosity reduction just happens near the injector. No significant oil saturation alteration in the reservoir and near the producer is observed.
- The influence of injection rate on the magnitude of the oil recovery is complex and depends on operational conditions of water injection and production. The favourable oil recovery is obtained at a high amount of both injection rate and temperature. Studying the effect of injection temperature and rate reveal that the oil recovery will increase due to oil viscosity reduction.
- Low permeability and porosity in a heavy oil reservoir considerably impact the enhanced oil recovery. While the oil recovery is less effective in reservoirs with higher permeability, it improves for the reservoir with higher porosity values.
- After 20 years of continuous hot water injection, less than 7% of the energy extracted from a geothermal doublet can be utilised to improve the oil recovery factor by 10% in an oil reservoir when the produced hot water from the oil production well is taken into account.
- For a homogeneous reservoir, the synergy between geothermal and stranded oil fields may reduce the required subsidy for a single doublet geothermal project up to 50%. Furthermore, if subsidy independence is the objective, scaling up the project to more doublets would be the best option in these kind of reservoirs; such configuration would not only reduce the required subsidy to zero but would potentially produce additional profit, making the synergy project attractive from an economic point of view.

Acknowledgment

The authors thank EBN for financial support of the project research of the first author. The first author also would further like to thank Mr. Liang Li for general assistance in programming in MATLAB.

References

[1] Van Heekeren V. The Netherlands country update on geothermal energy. Stichting Platform Geothermie, World Geothermal Congress; 2015.
[2] Bonté D, Van Wees JD, Verweij J. Subsurface temperature of the onshore Netherlands: new temperature dataset and modelling. Neth J Geosci 2012;91(04):491–515.
[3] Willems CJ, Nick HM, Donselaar ME, Weltje GJ, Bruhn DF. On the connectivity anisotropy in fluvial Hot Sedimentary Aquifers and its influence on geothermal doublet performance. Geothermics 2017;65:222–33.
[4] Farouq Ali SM. Heavy oil - evermore mobile. J Pet Sci Eng 2003;37:5–9.
[5] Teodoriu C, Falcone G, Espinel A. Letting off steam and getting into hot water - harnessing the geothermal energy potential of heavy oil reservoirs. In: Paper presented at the 20th world energy congress, Rome, Italy, 2007.
[6] Taber JJ, Martin FD, Serigth RS. EOR screening criteria revised – Part 1: introduction to screening criteria and enhanced recovery field projects. In: SPE 35385, WEA, SPE/DOE improved oil recovery symposium held in Tulsa, Oklahoma, 21–24 April, 1996.
[7] Milton BB, Nitzken JA. Controlling steam production in heat recovery steam generators for combined cycle and enhanced oil recovery operations. Power Gen International, Las Vegas, Nevada, December 9–11, 2003.
[8] Prats M. Thermal recovery. SPE Monogr 1986;7.
[9] Goodyear, Reynolds CB, Townsley PH, Woods CL. Hot water flooding for high permeability viscous oil fields. SPE-35373-MS, SPE/DOE improved oil recovery symposium, 21–24 April, Tulsa, Oklahoma; 1996.
[10] Bousaid IS. Hot-water and steamflood studies using kern river oil. International thermal operations symposium, Bakersfield, California 1991;vol. 21543.
[11] Jabbour C, Quintrad M, Betrin H, Robin M. Oil recovery by steam injection: three-phase flow effects. J Pet Sci Eng 1996;16:109–30.
[12] Okasha TM, Menouar HK, Abu-Khamsin SA. Oil recovery from tarmat reservoirs using hot water and solvent flooding. J Can Pet Technol 1998;37(4):33–40.
[13] Martin WL, Dew JN, Powers ML, Steves HB. Results of a tertiary hot waterflood in a thin sand reservoir. J Pet Technol 1968;739–750.
[14] Cassinat JC, Payette MC, Taylor DB, Cimolai MP. Optimizing waterflood performance by utilizing hot water injection in a high paraffin content reservoir. Improved oil recovery symposium, Tulsa, Oklahoma 2002;vol. 75141.
[15] Yu QT. Proceedings on oilfield development. Beijing: Petroleum Industry Press; 1999. p. 129–35.
[16] Pederson JM, Sitorus JH. Geothermal hot waterflood: Balam South Telisa Sand, Sumatra, Indonesia. SPE 2001;68724.
[17] Wang XZ, Wang JY. Study on feasibility of geothermal oil recovery in Gudong Oilfield. FaultBlock Oil Gas Field 2008;23(1):126–8.
[18] Chen T, Zhang Z, Liu Y. Experiment research on the impact of geothermal water temperature on heavy oil recovery factor. Special Oil Gas Reservoirs 2010;17(1):98–9. (in Chinese; 104).
[19] Macenic M, Kurevija T. Revitalization of abandoned oil and gas wells for a geothermal heat exploitation by means of closed circulation: case study of the deep dry well Pčelić-1. Interpretation 2018;6(1):SB1–9.
[20] Crooijmans RA, Willems CJL, Nick HM, Bruhn DF. The influence of facies heterogeneity on the doublet performance in low-enthalpy geothermal sedimentary reservoirs. Geothermics 2016;64:209–19.
[21] Mottaghy D, Pechnig R, Vogt C. The geothermal project Den Haag: 3D numerical models for temperature prediction and reservoir simulation. Geothermics 2011;40:199–210.
[22] Sanner B, Ria K, Land A, Mutka K, Papillon P, Stryi-Hipp G, et al. Common vision for the renewable heating & cooling sector in Europe. European Commission; 2011. [Technical report].
[23] Poulsen SE, Balling N, Nielsen SB. A parametric study of the thermal recharge of low enthalpy geothermal reservoirs. Geothermics 2015;53:464–78.
[24] Pujol M, Ricard LP, Bolton G. 20 years of exploitation of the Yarragadee aquifer in the Perth Basin of Western Australia for direct-use of geothermal heat. Geothermics 2015;57:39–55.
[25] Tureyen OI, Sarak H, Altun G, Satman A. A modeling analysis of unitized production: understanding sustainable management of single-phase geothermal resources with multiple lease owners. Geothermics 2015;55:159–70.
[26] Daniilidis A, Scholten T, Hooghiem J, De Persis C, Herber R. Geochemical implications of production and storage control by coupling a direct-use geothermal system with heat networks. Appl Energy 2017;204:254–70.
[27] Salimzadeh S, Nick HM, Zimmerman RW. Thermoporoelastic effects during heat extraction from low-permeability reservoirs. Energy 2018;142:546–58.
[28] Wys JN, Kimmell CE, Hart GF. The feasibility of recovering medium to heavy oil using geopressured geothermal fluids. Idaho: Prepared for US Department of Energy Field Office; 1991.
[29] Junrong L, Rongqiang L, Zhixue S. Exploitation and utilization technology of geothermal resources in oil fields. In: Proceedings world geothermal congress, Melbourne, Australia; 2015.
[30] Smits P. Construction of an integrated reservoir model using the Moerkapelle field for geothermal development of the Delft sandstone MS thesis Delft (The Netherlands): Delft University of Technology; 2008.
[31] EBN BV, Hoetz G, de Jong S. Synergie van stranded fields met geothermie & Geothermie mogelijkheden met olie/gas putten na productie; 2013.
[32] Ziabakhsh-Ganji Z, Donselaar ME, Bruhn DF, Nick HM. Thermally-enhanced oil recovery from stranded fields: synergy potential for geothermal and oil exploitation. European geothermal congress, Strasburg, France; 2016.
[33] Willems CJ, Nick HM, Weltje GJ, Bruhn DF. An evaluation of interferences in heat production from low enthalpy geothermal doublets systems. Energy 2017;135(15):500–12.
[34] Limberger J, Boxem T, Pluymaekers M, Bruhn DF, Manzella A, Calcagno P, et al. Geothermal energy in deep aquifers: a global assessment of the resource base for direct heat utilization. Renew Sustain Energy Rev 2018;82.
[35] Batzle M, Wang Z. Seismic properties of pore fluids. Geophysics 1992;57(11):1396–408.
[36] Kaya E, Zarrouk SJ, O'Sullivan MJ. Reinjection in geothermal fields: a review of worldwide experience. Renew Sustain Energy Rev 2011;15(1):47–68.
[37] Meyer RF, Steele CT, Olson JC. The future of heavy crude oils and tar sands: second international conference; 1984. p. 97–158 [chapter 16].
[38] Aziz K, Ramesh AB, Woo PT. Fourth SPE comparative solution project: comparison of steam injection simulators. SPE J Pet Technol 1987;39(12):1576–84.
[39] Scheidegger A. General theory of dispersion in porous media. J Geophys Res 1961;66(10):3273–8.
[40] Saeid S, Al-Khoury R, Nick HM, Barends F. Experimental–numerical study of heat flow in deep low-enthalpy geothermal conditions. Renew Energy 2014;62:716–30.
[41] Willems CJL, Nick HM, Goense T, Bruhn DF. The impact of reduction of doublet well spacing on the Net Present Value and the life time of fluvial Hot Sedimentary Aquifer doublets. Geothermics 2017;68:54–66.
[42] Ziabakhsh-Ganji Z, Kooi H. Sensitivity of Joule-Thomson cooling to impure CO_2 injection in depleted gas reservoirs. Appl Energy 2014;113:434–51.
[43] Hamouda AA, Karoussi O. Effect of temperature wettability and relative permeability on oil recovery from oil-wet chalk. Energies 2008;1:19–34.
[44] Bahadori A, Mahmoudi M, Nouri A. Prediction of heavy-oil viscosities with a simple correlation approach, SPE-157360-PA. Oil Gas Facilities 2014;4(01).
[45] Bahadori A, Vuthaluru HB. A novel correlation for estimation of hydrate forming condition of natural gases. J Nat Gas Chem 2009;18(4):453–7.
[46] Bahadori A. Determination of well placement and breakthrough time in horizontal wells for homogeneous and anisotropic reservoirs. J Petrol Sci Eng 2010;75(1–2):196–202.
[47] Bahadori A. Estimation of combustion flue gas acid dew point during heat recovery and efficiency gain. Appl Therm Eng 2011;31(8–9):1457–62.
[48] Nick HM, Schotting R, Gutierrez-Neri M, Johannsen K. Modeling transverse dispersion and variable density flow in porous media. Transp Porous Media 2009;78(1):11–35.
[49] Saeid S, Al-Khoury R, Nick HM, Hicks MA. A prototype design model for deep low-enthalpy hydrothermal systems. Renew Energy 2015;77:408–22.
[50] Wu B, Zhang X, Jeffrey RG, Bunger AP, Jia S. A simplified model for heat extraction by circulating fluid through a closed-loop multiple-fracture enhanced geothermal system. Appl Energy 2016;183:1664–81.
[51] Vik H, Salimzadeh S, Nick HM. Heat recovery from multiple-fracture enhanced geothermal systems: the effect of thermoelastic fracture interactions. Renew Energy 2018.
[52] Cheung KLH. SAGD well pair spacing evaluation with consideration of central processing facility constraints. SPE-165397-MS; 2013.
[53] Zhao DW, Wang J, Gates ID. Thermal recovery strategies for thin heavy oil reservoirs. Fuel 2014;117:431–41.
[54] Verney MJ. Evaluating SAGD performance due to changes in well spacing and length. SPE 174481-MS; 2015.
[55] Torabi F, Qazvini Firouz A, Crockett M, Emmons S. Feasibility study of hot waterflooding technique to enhance heavy oil recovery: investigation of the effect of well spacing, horizontal well configuration and injection parameters. In: SPE 157856. SPE heavy oil conference Canada held in Calgary, Alberta, Canada, 12–14 June 2012.
[56] Aramburo Velez DA. Synergy between geothermal and stranded oil fields to add value to geothermal projects MS thesis Delft (The Netherlands): Delft University of Technology; 2017.
[57] Energieonderzoek Centrum Nederland (ECN). Eindadvies Basisbedragen SDE +2017, Amsterdam; 2017.
[58] Van Wees JDAM, Kramers I, Kronimus RA, Pluymaekers MPD, Mijnlieff HF, Vis GJ. ThermoGis V1.0, Part II: methodology. 2010. TNO-Report.